

Molecularly self-assembled nucleic acid nanoparticles for targeted *in vivo* siRNA delivery

Hyukjin Lee^{1,4}, Abigail K. R. Lytton-Jean¹, Yi Chen¹, Kevin T. Love¹, Angela I. Park¹, Emmanouil D. Karagiannis¹, Alfica Sehgal⁵, William Querbes⁵, Christopher S. Zurenko⁵, Muthusamy Jayaraman⁵, Chang G. Peng⁵, Klaus Charisse⁵, Anna Borodovsky⁵, Muthiah Manoharan⁵, Jessica S. Donahoe⁶, Jessica Truelove⁶, Matthias Nahrendorf⁶, Robert Langer^{1,2,3} and Daniel G. Anderson^{1,2,3*}

Nanoparticles are used for delivering therapeutics into cells^{1,2}. However, size, shape, surface chemistry and the presentation of targeting ligands on the surface of nanoparticles can affect circulation half-life and biodistribution, cell-specific internalization, excretion, toxicity and efficacy³⁻⁷. A variety of materials have been explored for delivering small interfering RNAs (siRNAs)—a therapeutic agent that suppresses the expression of targeted genes^{8,9}. However, conventional delivery nanoparticles such as liposomes and polymeric systems are heterogeneous in size, composition and surface chemistry, and this can lead to suboptimal performance, a lack of tissue specificity and potential toxicity¹⁰⁻¹². Here, we show that self-assembled DNA tetrahedral nanoparticles with a well-defined size can deliver siRNAs into cells and silence target genes in tumours. Monodisperse nanoparticles are prepared through the self-assembly of complementary DNA strands. Because the DNA strands are easily programmable, the size of the nanoparticles and the spatial orientation and density of cancer-targeting ligands (such as peptides and folate) on the nanoparticle surface can be controlled precisely. We show that at least three folate molecules per nanoparticle are required for optimal delivery of the siRNAs into cells and, gene silencing occurs only when the ligands are in the appropriate spatial orientation. *In vivo*, these nanoparticles showed a longer blood circulation time ($t_{1/2} \approx 24.2$ min) than the parent siRNA ($t_{1/2} \approx 6$ min).

Self-assembled three-dimensional structures of short oligonucleotides have already been explored for imaging and delivery applications¹³⁻¹⁵. In this study we prepared oligonucleotide nanoparticles (ONPs) through programmable self-assembly of short DNA fragments and therapeutic siRNAs to develop a population of molecularly identical nanoparticles with controllable particle size and target ligand location and density. As shown in Fig. 1a, six DNA strands with complementary overhangs at the 3' ends can self-assemble into a tetrahedron consisting of 186 Watson-Crick base pairs. The six edges are each 30 base pairs long, and the theoretical tetrahedron height is ~ 8 nm with edges of 10 nm. Each edge contains a nick in the middle where the 5' and 3' ends of an oligonucleotide meet. The overhang at this nick is complementary to the overhang of siRNA strands. Thus, six siRNAs are bound per nanoparticle (one per edge). Chemically modified siRNA with

2'-OMe modifications (shown to significantly enhance serum stability as well as reduce the potential of immune stimulation) was used in our experiments¹⁶. Native polyacrylamide gel electrophoresis (PAGE) analysis was performed to demonstrate the stepwise assembly of DNA tetrahedron particles as each strand was added. A distinct band shift was observed, indicating DNA assembly, and yields of >95 and 98% were observed for tetrahedron formation and siRNA hybridization, respectively (Fig. 1b). The tetrahedron structure was imaged by atomic force microscopy (AFM) in aqueous buffer, and high-resolution images confirmed the presence of the three upper edges of an individual tetrahedron as well as a height of ~ 7.5 nm (Fig. 1c). Dynamic light scattering measured a hydrodynamic diameter of ~ 28.6 nm with a narrow size distribution, even when ONPs were prepared at a high concentration (8 μ M, Supplementary Fig. S1).

It has been suggested that the optimal particle size for a cancer-targeting nanodelivery carrier is 20–100 nm (refs 3,4,17). Nanoparticles with a diameter greater than 20 nm avoid renal clearance, which is a typical outcome for monomeric siRNA, and enhance delivery to certain tumour types through the enhanced permeability and retention effect (EPR)^{18,19}. In theory, ONPs are large enough to avoid renal filtration (>20 nm) but small enough to penetrate through the leaky vasculatures in a tumour region, bind to cell surface receptors and facilitate intracellular uptake, while reducing reticuloendothelial system (RES)-mediated clearance. Because ONPs are molecularly defined, they exist as a single uniform population in terms of size and shape. This is distinctly different from traditional cationic delivery carriers that can exist in a range of shapes and sizes. The nucleic acid composition of ONPs allows precise spatial control of all decorating ligands via hybridization, meaning that the siRNA component of the particle can be varied.

To ascertain whether ONPs can provide effective targeted delivery of siRNA to human cancer cells, we conjugated various cancer-targeting ligands from peptides to small molecules. It is hypothesized that intracellular delivery of ONPs will be promoted by active targeting of specific surface receptors on cancer cells^{20,21}. Among the 28 different targeting ligands tested here, folic acid (FA)-conjugated ONPs exhibited the greatest gene silencing, with $>50\%$ reduction of firefly luciferase expression in HeLa cells in a dose-dependent manner (Fig. 2a). A few cationic peptides (Hph-1 and Penetratin) also led to a reduction in firefly luciferase expression; however,

¹David H. Koch Institute for Integrative Cancer Research, Massachusetts Institute of Technology, Cambridge, Massachusetts 02139, USA, ²Department of Chemical Engineering, Massachusetts Institute of Technology, Cambridge, Massachusetts 02139, USA, ³Harvard-MIT Division of Health Science and Technology, Massachusetts Institute of Technology, Cambridge, Massachusetts 02139, USA, ⁴College of Pharmacy, Ewha Womans University, Seoul, Korea, ⁵Anylam Pharmaceuticals, Cambridge, Massachusetts 02142, USA, ⁶Center for Systems Biology, Massachusetts General Hospital and Harvard Medical School, Boston, Massachusetts 02114, USA. *e-mail: dgander@mit.edu

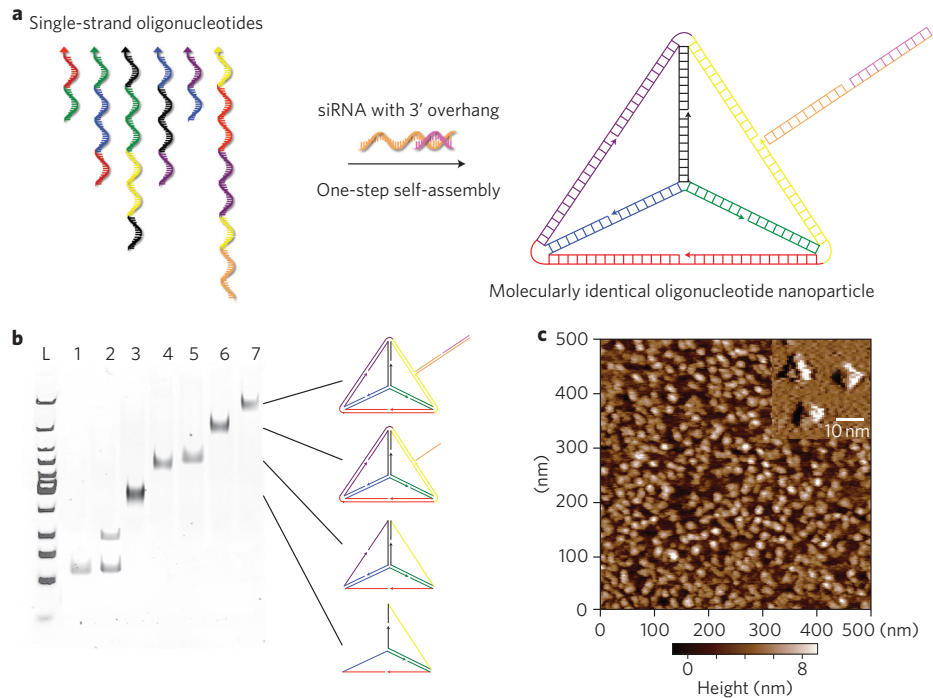


Figure 1 | Programmable self-assembly of ONPs. **a**, Schematic of DNA strands for tetrahedron formation (arrow head represents 5' end of the nucleic acid strand; each colour corresponds to one of the six edges of the tetrahedron) and representation showing site-specific hybridization of siRNA to the self-assembled nanoparticles. **b**, Native PAGE analysis to verify self-assembly of the DNA tetrahedron and hybridization of siRNAs to the DNA core, with the presumed structures schematically drawn on the right (Lane 1, strand 1; Lane 2, strands 1 and 2; Lane 3, strands 1-3; Lane 4, strands 1-4; Lane 5, strands 1-5; Lane 6, strands 1-6; Lane 7, strands 1-6 and siRNAs; Lane L, low-molecular-weight DNA ladder (see Supplementary Information for labelling)). **c**, AFM image showing monodisperse tetrahedron nanoparticles on mica. Colour bar indicates height in large image only. Inset: AFM image recorded in the amplitude channel with an ultrasharp tip, resolving the three upper edges of the tetrahedron.

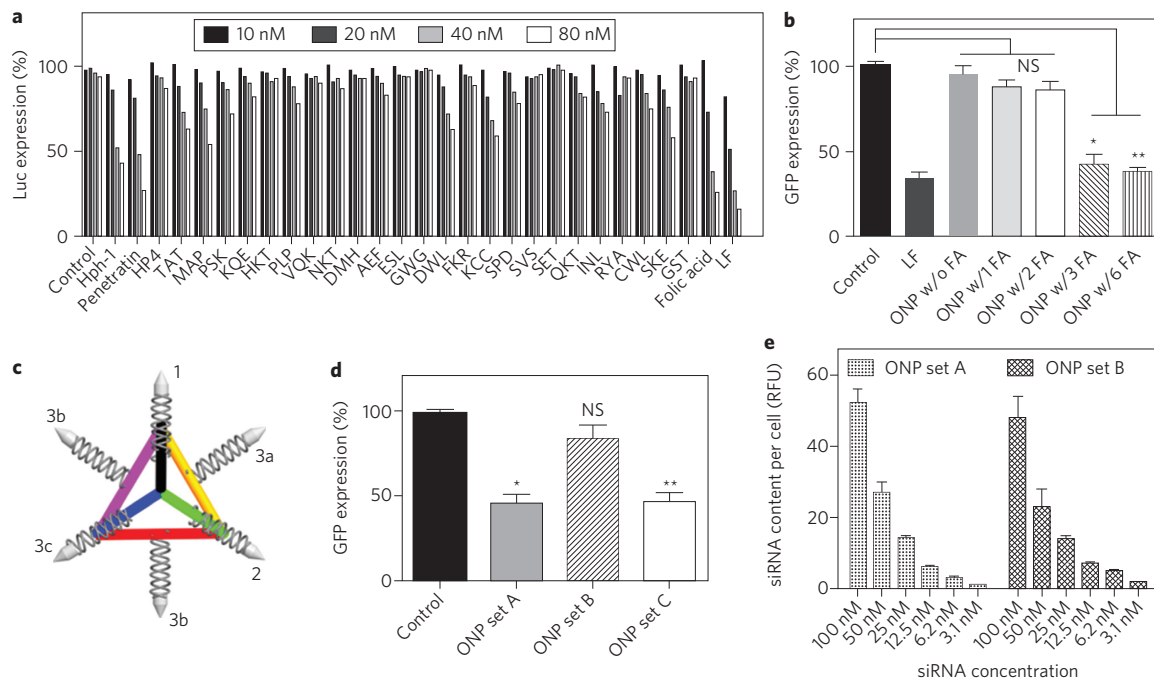


Figure 2 | In vitro screening and gene silencing using ONPs. **a**, Screening of tumour-targeting ligands using ONPs in a luciferase silencing assay in HeLa cells (control (ONPs without targeting ligands); LF (lipofectamine RNAiMax); peptide abbreviations are described in the Supplementary Information). **b**, GFP gene silencing efficiency varies with FA density on ONPs ($n = 4$; siRNA concentration, 35 nM). * $P < 0.003$, ** $P < 0.001$ compared with control (naked GFP siRNA). NS, not significant. **c**, Structure and orientation of the ligand (bullet shapes on ends of siRNA strands). **d**, Efficiency of gene silencing for ONPs ($n = 4$; siRNA concentration, 35 nM; set A, FA on 1, 2 and 3a; set B, FA on 1, 2 and 3b; set C, FA on 1, 2 and 3c). * $P < 0.018$, ** $P < 0.019$ compared with control (naked GFP siRNA). NS, not significant. **e**, Automated confocal analysis of intracellular uptake of ONPs with different FA orientations ($n = 8$). RFU, relative fluorescence units.

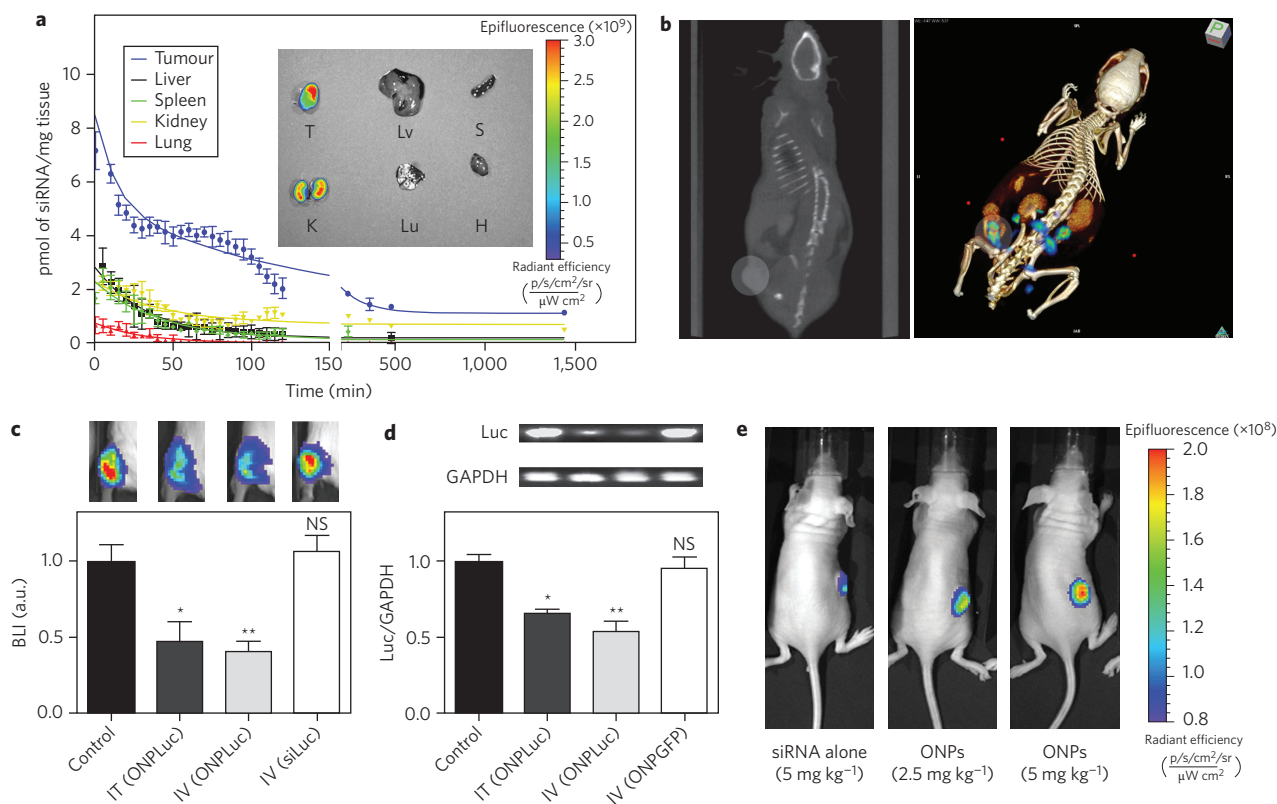


Figure 3 | *In vivo* pharmacokinetic profile and gene silencing in tumour xenograft mouse model. **a**, Pharmacokinetic profile of ONPs in KB tumour-bearing mice and *ex vivo* fluorescence image of five major organs and tumour 12 h post-injection (T, tumour; Lv, liver; S, spleen; K, kidney; Lu, lung; H, heart). A high level of siRNA accumulation occurs in tumour tissue. **b**, Tumour-specific accumulation of ONPs as determined by FMT-CT 25 min post-injection (left, CT scan; right, three-dimensional FMT-CT). The highlighted circular region indicates the location of the tumour xenograft. Warmer colours in the tumour region represent site-specific accumulation of Cy5-labelled ONPs. **c**, *In vivo* luciferase silencing in KB tumour xenografts ($n = 7$; BLI, bioluminescence intensity; control, PBS injection; IT, intratumoral; IV, intravenous; ONPLuc, ONPs with folate-conjugated anti-luciferase siRNA; siLuc, folate-conjugated anti-luciferase siRNA). siRNA concentration, 2.5 mg kg^{-1} . $*P < 0.138$, $**P < 0.002$ compared with control. NS, not significant. The four images above the bar graph are live BLI images of mice from each group. Warmer colours indicate strong BLI in the tumour xenografts. **d**, Quantitative analysis of luciferase mRNA expression in KB tumours two days after ONP injection ($n = 3$; control (PBS injection); ONPLuc (ONPs with folate-conjugated anti-luciferase siRNA); ONPGFP (ONPs with folate-conjugated anti-GFP siRNA); Luc). siRNA concentration, 2.5 mg kg^{-1} . Luc is a firefly luciferase gene. GAPDH is used as a house keeping gene. Luciferase mRNA level is expressed as a ratio with GAPDH (Luc/GAPDH). $*P < 0.05$, $**P < 0.03$ compared with control. NS, not significant. **e**, *In vivo* live fluorescence images showing dose-responsive accumulation of ONPs in KB tumours compared with FA-conjugated siRNA (siRNA alone); animals were treated by systemic injection ($n = 3$) and images are representative of each group.

the structures of the ONPs modified with these ligands were less stable, causing unwanted aggregation due to the charge interaction between the cationic peptides and anionic nucleic acids. For folate-mediated gene silencing, folate receptor overexpressing KB cells (expressing green fluorescent protein, GFP) were also tested to confirm the specificity of the targeted gene silencing. Our data showed a reduction of $>60\%$ in GFP expression in KB cells at a 35 nM dose of FA-conjugated ONPs carrying siRNA-targeting GFP (Supplementary Fig. S2).

In addition to their optimal particle size and cancer specificity for intracellular siRNA delivery, ONPs allow full control of the spatial orientation of ligands as well as the density of ligands on the nanoparticle surface. Because the geometry of the ONPs is well defined, it is possible to investigate correlations of ligand density and orientation with gene silencing. To evaluate the importance of spatial orientation for the targeting ligand, six different overhang sequences were designed for siRNA hybridization and the number of hybridized siRNAs was varied as well as the density and location of the folate. We can specifically control the number of siRNAs on the core DNA tetrahedron to between one and six (Supplementary Fig. S3). By using both FA-conjugated and non-conjugated siRNAs, the level of GFP gene silencing was

investigated with various numbers of folate ligands, while maintaining the same number of siRNAs on each nanoparticle (Fig. 2b). Our results indicate that a minimum of three folate ligands are required to achieve GFP gene silencing. Interestingly, having more than three ligands on one particle did not improve gene silencing efficiency. Importantly, the orientation/location of the ligands dramatically affects gene silencing (Fig. 2d). When three FAs were decorated on the tetrahedron so that the local density was maximized (three folates encompass a face or vertex of the tetrahedron: example locations are 1, 2 and 3a or 1, 2 and 3c in Fig. 2c, respectively), GFP silencing was observed. However, when three FAs were located at a greater distance from one another on the tetrahedron so that the local density was lower (locations 1, 2 and 3b), we did not observe any GFP silencing. Our confocal study revealed that the intracellular uptakes of these nanoparticles were similar, regardless of FA location (Fig. 2e); however, potent gene silencing activity was only observed for nanoparticles with the appropriate spatial orientation of FA (Fig. 2d). It is conceivable that, with a specific orientation of FA, the higher local ligand density may influence the intracellular trafficking pathway of nanoparticles through the cells and corresponding gene silencing. Although it is believed that the density and location of ligands can greatly influence

nanoparticle–cell membrane interactions as well as intracellular uptake pathways, this phenomenon is extremely difficult to prove using conventional nanoparticles due to the lack of precise control of ligand density and orientation on a single nanoparticle^{22,23}.

To verify *in vivo* delivery of ONPs, the pharmacokinetic profile and organ biodistribution were investigated in nude mice bearing KB xenograft tumours. Cy5-labelled ONPs with folate ligands (3 nmol siRNA, ~ 2.0 mg kg⁻¹; six FA ligands per ONP) were systemically delivered by tail-vein injection, and *in vivo* behaviour was quantitatively measured over the course of 24 h by fluorescence molecular tomography fused with computed tomography (FMT-CT)^{24,25}. Co-registration of FMT and CT provided high-resolution fluorescence images of tumour targeting by the ONPs and the distribution of nanoparticles in five major organs. As shown in Fig. 3a, ONPs accumulated primarily in the tumour and kidney, with little accumulation in other organs such as liver, spleen, lung and heart. *Ex vivo* fluorescence images at 12 h post-injection also correspond well with the biodistribution data. A reconstructed three-dimensional FMT-CT image of a tumour-bearing mouse revealed accumulation of ONPs in the tumour region as early as 25 min post-injection (Fig. 3b). Also, the blood half-life data indicate that ONPs have a longer blood circulation time ($t_{1/2} \approx 24.2$ min) than the parent siRNA ($t_{1/2} \approx 6$ min; Supplementary Fig. S4)²⁶.

To assess the therapeutic potential of ONPs as cationic-free gene delivery carriers, we conducted *in vivo* gene silencing of firefly luciferase expressing KB xenografts. FA-conjugated ONPs with anti-luciferase siRNA were administered at a dose of 2.5 mg kg⁻¹ of siRNA into mice, either by tail-vein injection or intratumour injection. Silencing was evaluated 48 h post-injection by measuring bioluminescent intensity in the tumour (Fig. 3c). Both tail-vein and intratumour injections resulted in a decrease of $\sim 60\%$ in bioluminescent intensity. When mice were injected by either mode of administration with FA-conjugated anti-luciferase siRNAs (not assembled into nanoparticles), no decrease in bioluminescent intensity was observed. This result corresponds well with our *in vitro* silencing experiment, confirming that the ONPs are a critical factor for successful gene silencing. Furthermore, measurement of the firefly luciferase mRNA level in tumour cells strongly supported target-specific mRNA cleavage by both systemic and local delivery of ONPs (Fig. 3d). A dose-dependent study revealed that tumour-specific accumulation of ONPs was achieved by systemic delivery (Fig. 3e), and the half-maximum inhibitory concentration (IC₅₀) for luciferase silencing was estimated to be ~ 1.8 mg kg⁻¹ (Supplementary Fig. S5a). Finally, the immune response of ONPs was monitored by measuring the IFN- α levels in blood samples 6 h post-injection. There was no significant increase in IFN- α compared to levels in untreated mice (Supplementary Fig. S5b).

This study has demonstrated that six single-stranded DNA fragments, and six double-stranded siRNAs, can self-assemble in a one-step reaction to generate DNA/siRNA tetrahedral nanoparticles for targeted *in vivo* delivery. The overhang design of the DNA strands allows specific hybridization of complementary siRNA sequences and provides full control over the spatial orientation of the siRNA and the locations and density of cancer-targeting ligands. The ONPs can be modified with different tumour-targeting ligands by simple conjugation chemistry, extending the use of these nanoparticles to the treatment of various cancers. We observed robust gene silencing with both intratumour and systemic injection of ONPs into KB xenograft tumours, without any detectable immune response. We believe these particles may also have utility in the treatment of other tissues by modification of their size and ligand type.

Methods

Preparation of self-assembled DNA/siRNA nanoparticles (ONPs). Six single-stranded DNAs (IDT) and six double-stranded siRNAs (Alnylam) were annealed to prepare ONPs. DNA strands (final strand concentration, 3.3 μ M each) were mixed

in an equal molar ratio in 2X PBS containing 300 mM NaCl, and a sixfold molar excess of siRNA strands was added to the solution. The solution was heated to 90 °C for 2 min and rapidly cooled to 4 °C to generate ONPs (particle concentration, 3.3 μ M). For FA-conjugated ONPs, FA-conjugated luciferase or GFP siRNA (Alnylam) was used. All siRNAs were chemically modified with site-specific 2'-Ome chemistry to avoid immune response activation and to improve nuclease resistance²⁶.

***In vitro* testing of ONPs.** HeLa cells, modified to stably express both firefly and Renilla luciferase genes, were used for *in vitro* screening of the ONPs. ONPs with different ligands were applied to 1.5×10^4 HeLa cells in medium containing serum. Firefly luciferase silencing was assessed 24 h post-transfection using a Dual-Glo Luciferase Assay kit (Promega). Transfections were performed in quadruplicate. siRNA transfected into cells using Lipofectamine RNAiMax (Invitrogen) was used as a positive control (Fig. 2). For folate receptor targeted GFP gene silencing, GFP-expressing KB cells were used. The level of GFP silencing was evaluated 24 h post-transfection using a BD FACSCalibur.

siRNA delivery in mice using ONPs. All animal experiments were conducted using institutionally approved protocols. Luc-KB tumour-bearing female BALB/c nude mice (Charles River Laboratories) received tail-vein or intratumour injections of either PBS (negative control) or ONPs containing anti-Luc siRNA diluted in PBS ($n = 7$ for each group; siRNA concentration, 2.5 mg kg⁻¹). Two days post-injection, bioluminescence intensity (BLI) in KB tumours was measured using an IVIS Lumina imaging system.

Full Methods and any associated references are available in the online version of this Letter at www.nature.com/naturenanotechnology.

Received 31 October 2011; accepted 17 April 2012;
published online 3 June 2012

References

- Panyam, J. & Labhasetwar, V. Biodegradable nanoparticles for drug and gene delivery to cells and tissue. *Adv. Drug Deliv. Rev.* **55**, 329–347 (2003).
- Peer, D. *et al.* Nanocarriers as an emerging platform for cancer therapy. *Nature Nanotech.* **2**, 751–760 (2007).
- Petros, R. A. & DeSimone, J. M. Strategies in the design of nanoparticles for therapeutic applications. *Nature Rev. Drug Discov.* **9**, 615–627 (2010).
- Choi, H. S. *et al.* Design consideration for tumour-targeted nanoparticles. *Nature Nanotech.* **5**, 42–47 (2010).
- Weissleder, R., Kelly, K., Sun, E. Y., Shtatland, T. & Josephson, L. Cell-specific targeting of nanoparticles by multivalent attachment of small molecules. *Nature Biotechnol.* **23**, 1418–1423 (2005).
- De Jong, W. H. & Borm P. Drug delivery and nanoparticles: applications and hazards. *Int. J. Nanomed.* **3**, 133–149 (2008).
- Akinc, A. *et al.* Targeted delivery of RNAi therapeutics with endogenous and exogenous ligand-based mechanisms. *Mol. Ther.* **18**, 1357–1364 (2010).
- Elbashir, S. M. *et al.* Duplexes of 21-nucleotide RNAs mediate RNA interference in cultured mammalian cells. *Nature* **411**, 494–498 (2001).
- Bumcrot, D., Manoharan, M., Kotliansky, V. & Sah, D. W. Y. RNAi therapeutics: a potential new class of pharmaceutical drugs. *Nature Chem. Biol.* **2**, 711–719 (2006).
- Whitehead, K. A., Langer, R. & Anderson, D. G. Knocking down barriers: advances in siRNA delivery. *Nature Rev. Drug Discov.* **8**, 129–138 (2009).
- Oh, Y. K. & Park, T. G. siRNA delivery systems for cancer treatment. *Adv. Drug Deliv. Rev.* **61**, 850–862 (2009).
- Lv, H., Zhang, S., Wang, B., Cui, S. & Yan, J. Toxicity of cationic lipids and cationic polymers in gene delivery. *J. Control. Rel.* **114**, 100–109 (2006).
- Bhatia, D. *et al.* A synthetic icosahedral DNA-based host–cargo complex for functional *in vivo* imaging. *Nature Commun.* **2**, 339 (2011).
- Walsh, A. S., Yin, H., Erben, C. M., Wood, M. J. A. & Tuberfield, A. J. DNA cage delivery to mammalian cells. *ACS Nano* **5**, 5427–5432 (2011).
- Keum, J. W., Ahn, J. H. & Bermudez, H. Design, assembly, and activity of antisense DNA nanostructures. *Small* **7**, 3529–3535 (2011).
- Gaglione, M. & Messere, A. Recent progress in chemically modified siRNAs. *Mini Rev. Med. Chem.* **10**, 578–595 (2010).
- Davis, M. E., Chen, Z. & Shin, D. M. Nanoparticle therapeutics: an emerging treatment modality for cancer. *Nature Rev. Drug Discov.* **7**, 771–782 (2008).
- Allen, T. M. & Cullis, P. R. Drug delivery systems: entering the mainstream. *Science* **303**, 1818–1822 (2004).
- Mok, H., Lee, S. H., Park, J. W. & Park, T. G. Multimeric small interfering ribonucleic acid for highly efficient sequence-specific gene silencing. *Nature Mater.* **9**, 272–278 (2010).
- Song, E. *et al.* Antibody mediated *in vivo* delivery of small interfering RNAs via cell-surface receptors. *Nature Biotechnol.* **23**, 709–717 (2005).
- Li, S. D., Chen, Y. C., Hackett, M. J. & Huang, L. Tumor-targeted delivery of siRNA by self-assembled nanoparticles. *Mol. Ther.* **16**, 163–169 (2008).

22. Tarapore, P., Shu, Y., Guo, P. & Ho, S. M. Application of Phi29 motor pRNA for targeted therapeutic delivery of siRNA silencing metallothionein-IIA and surviving in ovarian cancers. *Mol. Ther.* **19**, 386–394 (2011).
23. Manz, B. N. *et al.* T-cell triggering thresholds are modulated by the number of antigen within individual T-cell receptor clusters. *Proc. Natl Acad. Sci. USA* **108**, 9089–9094 (2011).
24. Nahrendorf, M. *et al.* Hybrid PET-optical imaging using targeted probes. *Proc. Natl Acad. Sci. USA* **107**, 7910–7915 (2010).
25. Leuschner, F. *et al.* Therapeutic siRNA silencing in inflammatory monocytes in mice. *Nature Biotechnol.* **29**, 1005–1010 (2011).
26. Soutschek, J. *et al.* Therapeutic silencing of an endogenous gene by systemic administration of modified siRNAs. *Nature* **432**, 173–178 (2004).

Acknowledgements

This work was supported by the National Institutes of Health (EB000244), the Center for Cancer Nanotechnology Excellence (U54 CA151884), Alnylam Pharmaceuticals and the

National Research Foundation of Korea (NRF-2011-357-D00063). The authors thank J. Hong and C. Hong for figure drawing, and J.B. Lee and A. Schroeder for helpful discussions.

Author contributions

H.L., A.L.J. and D.G.A. planned the experiments. H.L., A.P., K.L., A.S., W.Q., C.Z., J.S.D., A.L.J. and J.T. conducted the experiments. H.L., A.L.J., Y.C., K.L., E.D.K., M.N., R.L. and D.G.A. analysed the data. H.L., A.L.J., M.M. and D.G.A. wrote the paper.

Additional information

The authors declare no competing financial interests. Supplementary information accompanies this paper at www.nature.com/naturenanotechnology. Reprints and permission information is available online at <http://www.nature.com/reprints>. Correspondence and requests for materials should be addressed to D.G.A.

Molecularly Self-Assembled Nucleic Acid Nanoparticles for Targeted In Vivo siRNA Delivery

Hyukjin Lee^{1,4}, Abigail K. R. Lytton-Jean¹, Yi Chen¹, Kevin T. Love¹, Angela I. Park¹, Emmanouil D. Karagiannis¹, Alfica Sehgal⁵, William Querbes⁵, Christopher S. Zurenko⁵, Muthusamy Jayaraman⁵, Chang G. Peng⁵, Klaus Charisse⁵, Anna Borodovsky⁵, Muthiah Manoharan⁵, Jessica S. Donahoe⁶, Jessica Truelove⁶, Matthias Nahrendorf⁶, Robert Langer^{1,2,3}, and Daniel G. Anderson^{1,2,3*}

* To whom correspondence should be addressed. E-mail: dgander@mit.edu

This document file includes:

Material and Methods

Figs. S1 to S5

References

Supporting online material for

Molecularly Self-Assembled Nucleic Acid Nanoparticles for Targeted In Vivo siRNA Delivery

Hyukjin Lee^{1,4}, Abigail K. R. Lytton-Jean¹, Yi Chen¹, Kevin T. Love¹, Angela I. Park¹, Emmanouil D. Karagiannis¹, Alfica Sehgal⁵, William Querbes⁵, Christopher S. Zurenko⁵, Muthusamy Jayaraman⁵, Chang G. Peng⁵, Klaus Charisse⁵, Anna Borodovsky⁵, Muthiah Manoharan⁵, Jessica S. Donahoe⁶, Jessica Truelove⁶, Matthias Nahrendorf⁶, Robert Langer^{1,2,3}, and Daniel G. Anderson^{1,2,3*}

* To whom correspondence should be addressed. E-mail: dgander@mit.edu

This document file includes:

Material and Methods

Figs. S1 to S5

References

Materials and Methods

Oligonucleotides

Sequence design was modified from Goodman et al. to have 30 bp on each side of the tetrahedral nanoparticle along with an overhang for siRNA hybridization¹. Subsequences corresponding to the edges of the tetrahedron are identified by the following color code, consistent with that used in Fig. 1A. Each DNA strand has an additional overhang sequences on the 3' end (OH for all other experiment, except for ligand density study for Fig. 3).

DNA strands for tetrahedron formation

S1: 5'-GTCTGAGGCAGTTGAGAGATCTCGAACATTCC-Overhang-3'

S2: 5'-TAAGTCTGAAGATCCATTTATCACCAGCTGCTGCACGCCATAGTAGCGTATCACCTGTCC- Overhang -3'

S3: 5'-AGCTACTTGCTACACGAGGATCTTCAGACTTAGGAATGTTTCGAGATCATGCGAGGACTCGGTCCAATACCGTACTAACGATTACAGATCAA-Overhang -3'

S4: 5'-CAGCTGGTGATAAAACGTGTAGCAAGTAGCTTTGATCTGTAATCGACTCTACGGGAAGAGC- Overhang -3'

S5: 5'-ATGCCCATCCGGCTCACTACTATGGCGTGCAG- Overhang -3'

S6: 5'-CGAGTCTCGCATGACTCAACTGCCTCAGACGGACAGGTGATACGAGAGCCGGATGGGCATGCTCTCCCGTAGAGATAGTACGGTATTGGAC-Overhang -3'

Overhang design

General overhang sequence for in vivo study, T color coding of the DNA strands indicates regions of complementarity. For all experiments except those in Figure 3, the overhangs above had the sequence,
5'-TTT TTT TTT TTT TTT TTT TTT-3'

For the ligand density study, (Figure 3), six different overhang sequences were used:

- 1: 5'-ATC GTA CGA TCA TAG ATC AAT-3'
- 2: 5'-TAC AGT CGT ATT GCA TTC CGA-3'
- 3: 5'-ATT CTA GAC GTT ACT TAA CAT-3'
- 4: 5'-TAA CTA TAG CTA CAA GCT TTC-3'
- 5: 5'-CCA TAC CGC CAT TTC CAA CTA-3'
- 6: 5'-AAG CAC ATG CGA TGT TTA ACT-3'

List of targeting ligands used in vitro screening

a. Cationic peptides

1. Hph-1: protein transduction domain peptide from human transcriptional factor

YARVRRRGPRRGGC

2. Penetratin: peptide from DNA binding domain of homeoproteins

RQIKIWFQNRRMKWKKC

3. HP4: Sperm histone peptide

RRRRPRRRTRRRRC

4. TAT: HIV peptide

GRKKRRQRRRPPQC

b. Amphipathic peptides

MAP: KLALKLALKALKALKLAC

c. Zwitterionic peptides

1. PSK: PSKDAFIGLM

2. KQE: KQEEETHIRNEQVRQRAKECSQALSLIDIDHG

3. HKT: HKTDSFVGLM

4. PLP: PLPLLILGSLLMTPPVIQAIHDAQR

5. VQK: VQKFPWWWPFLKK

6. NKT: QKTVEGAGSIAAATG

7. DMH: DMHDFVGLM

8. AEF: AEFLKVFLPSLLLSHLLAIGLGIYIG
9. ESL: ESLSGVCEISGRLYRLCCR
10. GWG: GWGSFFKKAHVGVKGVGKAALTHYL
11. DWL: DWLKAFYDKVAEKLKEAF
12. FRK: FKRTADGRCKPTF
13. KCC: GCCSYPPCFATNPDC
14. SPD: SPDEREWMRAIQMVANSLK
15. SVS: GVSELLISTAVQGILFALLGA
16. SET: SETLYTESRKLLRSWHLPSV
17. QKT: QKTVEGAGSIAAATG
18. INL: INLKALAALAKKIL
19. RYA: RWCYAYVVRIRGVLVRYRRCW
20. CWL: CWLCRALIKRIQAMIP
21. SKE: SKEWQPAQVILL
22. GST: GSTLYTESRKLLRSWHLPSV

d. Small molecules

Folic Acid

e. Commercial lipid carrier

LF: Lipofectamine RNAiMax (Invitrogen)

siRNA sequences for gene silencing

anti-Luc siRNA

sense: 5'-**Cy5**-AAcGcuGGGcGuuAAucAAdTdT-**Folate**-3'

antisense: 5'-UUGAUuAACGCCcAGCGUuTdT-**overhang^c**-3'

anti-GFP siRNA

sense: 5'- **Cy5**-AcAuGAAGcAGcACGACuUdTdT-**Folate**-3'

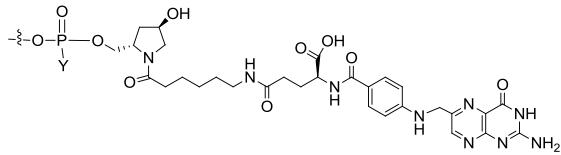
antisense: 5'-AAGUCGUGCUGCUUCAUGUdTdT-**overhang^c**-3'

nomenclature: lower case letters = 2'Omethyl modified RNA nucleotide

overhang^c = 5'-AAA AAA AAA AAA AAA AAA AAA-3'

The overhang is composed of (dA)₂₀ resulting in a DNA/RNA chimera

Folate was conjugated to RNA at the 3'-end using a hydroxyprolinol scaffold where the prolinol amino group was conjugated to the α -COOH of folic acid with an extended aminocaproic acid tether:



Self-assembly of tetrahedron DNA/siRNA nanoparticles (ONPs).

Stoichiometric mixtures of component oligonucleotides (single-stranded DNA and double-stranded siRNA) were combined in TM buffer (10 mM Tris, 5 mM MgCl₂), heated to 95°C for 2 minutes, then rapidly cooled to 4°C in an Eppendorf Mastercycler Personal machine. Particle size of ONPs was determined in PBS using a ZETAPals analyzer (Brookhaven Instruments, Holtsville, NY).

Quantification

To quantify self-assembly yields, tetrahedron DNA nanoparticles with/without siRNA were run on a PAGE gel (5% TBE Ready Gels, Bio-Rad) with 1x TBE buffer and stained with SYBR Gold (Invitrogen). Band intensities were quantified with Image Lab software (Bio-Rad). Yields were estimated to be > 95% for tetrahedron formed from 1 μ M stock component oligonucleotides and > 98% for siRNA hybridization, respectively.

AFM imaging

ONPs, diluted to 10 nM in TM buffer supplemented with 10 mM NiCl₂ in a 10- μ l volume, were incubated for 15 minutes on freshly cleaved mica. After 15 minutes, buffer was added to a total volume of 200 μ l and the sample was scanned in an MFD-3D atomic force microscope (Asylum Research, USA) operated in AC mode. Cantilever type: For general scanning, a BL-AC40TS (Olympus Inc., Japan) microscope was used. For the high-resolution images, an SNL-10 (Veeco Inc., USA) with super-sharp tips of 2-3 nm radius was used.

Automated confocal microscopy

GFP expressing KB cells were seeded at 2.0×10^4 cells/well in black 96-well plates with clear bottom (Corning, NY). Cells were incubated with various concentrations (3.1 to-100 nM) of ONPs containing cy5 fluorophore for 24 h at 37°C. Cells were washed with PBS then counter-stained in PBS-containing Hoescht (2 µg/ml) for nuclei identification. Stained live cell imaging was performed with an automated spinning disk confocal microscope (OPERA; Perkin Elmer, Shelton, CT) with a ×40 objective. The same defined pattern of 20 fields from each well was acquired to eliminate bias and provide a statistically significant number of cells for analysis. After identification of cell location and perimeter, siRNA content per each cell was calculated as well as the intensity of endogenous GFP using Acapella software. Data presented are an average of intracellular intensity from 20 different fields.

Preparation of Luc-KB tumor bearing mice

All animal care and experimental procedures were conducted using institutionally approved protocols. For *in vivo* optical imaging, a xenograft tumor was generated by subcutaneous injection of firefly Luc expressing KB cells (2×10^6 cells/mouse) into a flank region of female nude mice (BALB/c). Tumor bearing mice were used when the diameter of tumors reached 6-8 mm.

***In vivo* FMT-CT**

CT and FMT imaging was done while the anesthetized mice were restrained in a dedicated multi-modal imaging cassette (dimensions 50 × 30 × 280 mm; VisEn Medical). The nontransparent body of the cassette has an adjustable height to accommodate mice of different sizes and holds two transparent acrylic windows that allow laser excitation and photon emission in trans-illumination geometry during FMT imaging. During imaging, mice were anesthetized (isoflurane 1.5%, O₂ 2L/min). An isoflurane delivery system is integrated into the multi-modal imaging cassette. Cy5-labeled ONPs were administered via tail-vein injection (3 nmol per mouse). We acquired 30 frontal slices of 0.5 mm thickness in the z direction, with an in-plane resolution of 1 × 1 mm. Time course images were taken every 5 min for 2 h, and then images were taken at 4, 6, 8, and 24 h post-injection. After image acquisition, datasets were post-processed using a normalized Born forward equation to calculate fluorochrome concentration, expressed in nM fluorescence per voxel, as described previously².

mRNA assay for tumor implants

The cellular level of firefly *luciferase* mRNA was analyzed by a reverse transcriptase-polymerase chain reaction (RT-PCR). The tumor implants were collected from mice 2 days post-injection of ONPs (n=3). Tissue samples were homogenized and total RNA was isolated using Trizol reagent (Invitrogen, Carlsbad, CA) according to the manufacturer's protocol. Quantitative RT-PCR was performed with the purified total RNA (1 µg) using SuperScript™ III One-Step RT-PCR system with Platinum *Taq* DNA polymerase (Invitrogen, Carlsbad, CA). The real time PCR was performed as previously described³. The PCR primers to detect firefly luciferase and GAPDH were obtained from IDT (Chicago, IL).

Forward: TCC AAC ACC CCA ACA TCT TC

Reverse: GTC TTT CCG TGC TCC AAA AC

Probe: /56-FAM/AGA CCT GCG ACA CCT GCG T/36-TAMSp/

The PCR products were also analyzed by 2% agarose gel electrophoresis and visualized by SYBR gold (Invitrogen) staining.

IFN- α ELISA for early immune response

To evaluate early immune responses *in vivo*, plasma IFN- α levels was determined using female C57BL/6 mice (Charles River Laboratory, Wilmington, MA). All mice were 7 weeks old and 20-25 g in body weight at the time of injection. Each of three mice was intravenously injected with siRNAs/Lipofectamine polyplexes or ONPs (2.5 mg/kg dose) in a 200 μ l injection volume. Control mice were injected with PBS solution. After 6 h incubation, blood samples were collected from the mice and plasma IFN- α levels were analyzed by an ELISA kit (PBL Biomedical, Piscataway, NJ).

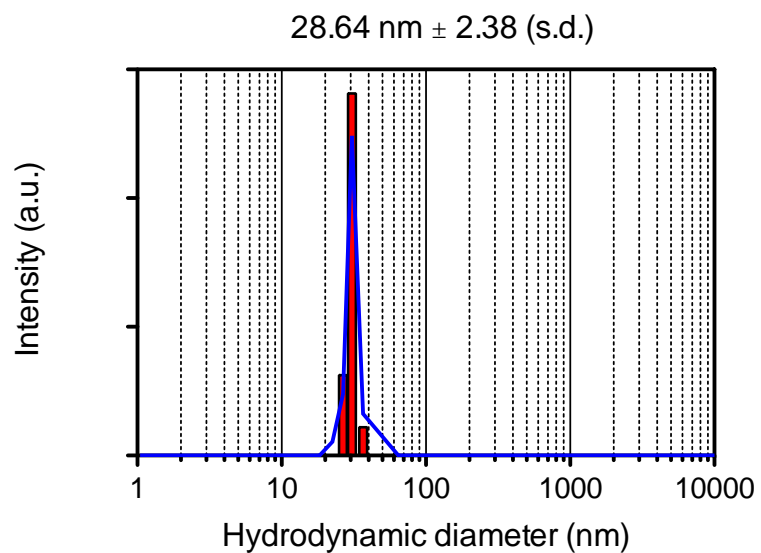


Figure S1 | Particle size measurement of self-assembled oligonucleotide nanoparticles (ONPs). DLS data showing monodisperse size distribution of ONPs with six siRNAs via simple hybridization (n =5): Mean hydrodynamic diameter is shown above as well as the standard deviation. There is no difference in size when the ONPs are prepared at low (blue line: 0.16 μ M) and high (red bar: 8 μ M) concentration, confirming the high self-assembly efficiency as well as the stability of ONPs.

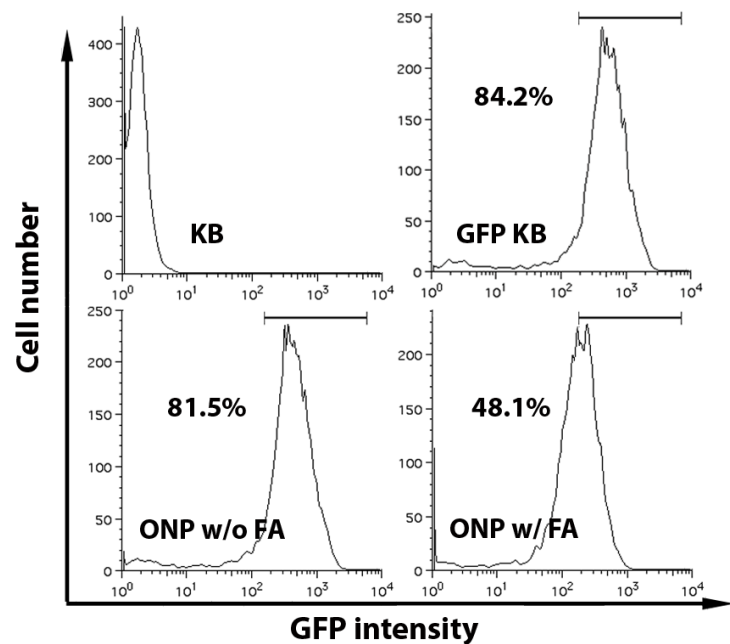


Figure S2 | Folate mediated gene silencing using KB cells. Flow cytometry analysis of GFP gene silencing in GFP-KB cells by folate conjugated ONPs (KB: GFP negative KB, GFP-KB: GFP positive KB, ONP w/o FA: ONPs with anti-GFP-siRNA, ONP w/ FA: ONPs with folate conjugated anti-GFP-siRNA, siRNA concentration = 35 nM). The number means the percentage of GFP-overexpressing cells sorted within a prefixed gate region as indicated by a bar. Compared to ONPs without FA, FA conjugated ONPs result in efficient GFP gene silencing in KB cells.

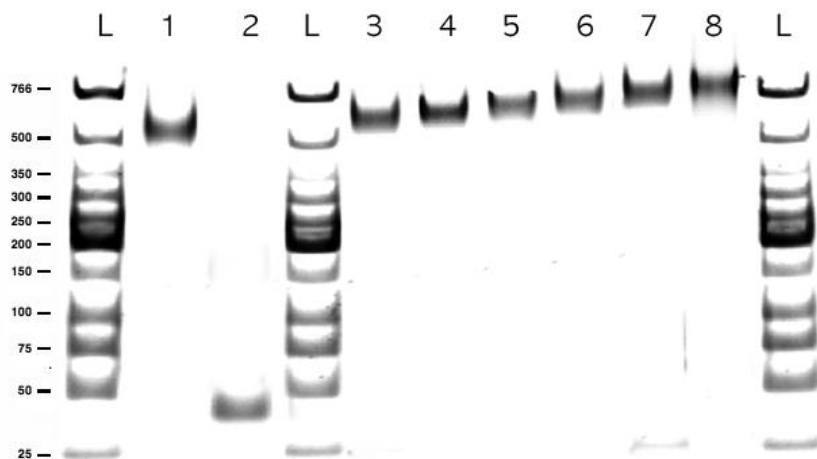


Figure S3 | Full control of siRNA hybridization on DNA tetrahedron. PAGE analysis of the full control of siRNA density on DNA tetrahedron (Lane 1: DNA tetrahedron, Lane 2: siRNA, Lane 3: DNA tetrahedron with 1 siRNA, Lane 4: with 2 siRNAs, Lane 5: with 3 siRNAs, Lane 6: with 4 siRNAs, Lane 7: with 5 siRNAs, Lane 8: with 6 siRNAs, L stands for low molecular weight DNA ladder: MW of each bands are shown on left). As the number of siRNA hybridization increases, a distinct band shift is observed due to the mobility change. Different overhang designs for site-specific siRNA hybridization allows precise control of siRNA density as well as presenting targeting ligands in a specific orientation.

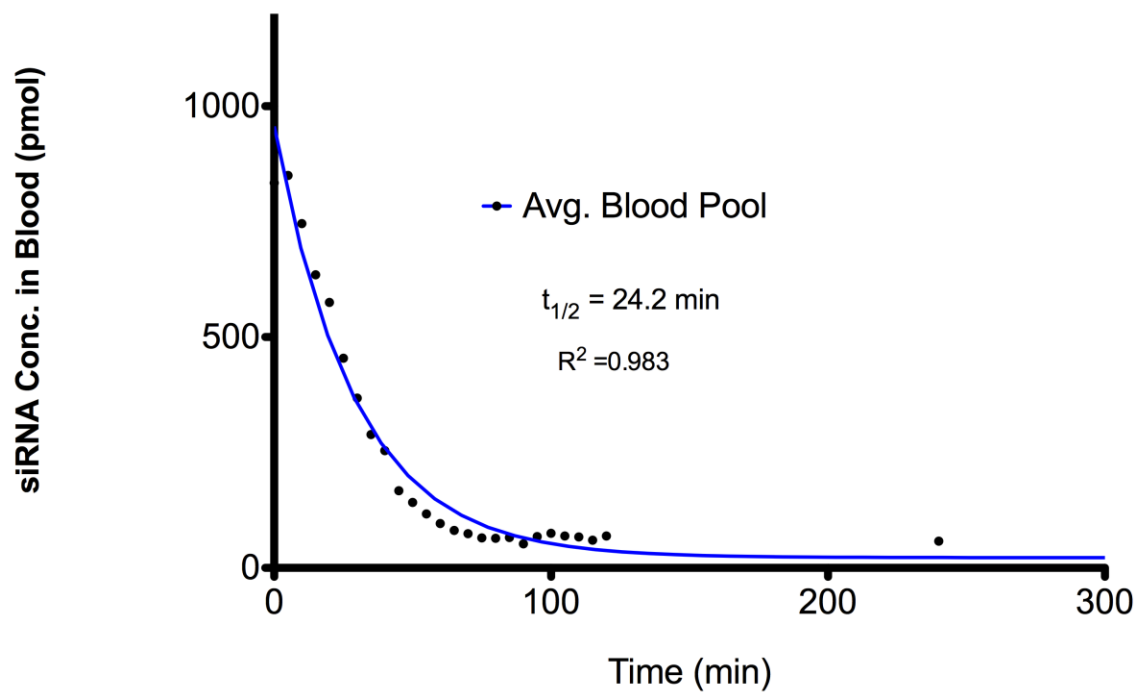


Figure S4 | Pharmacokinetic of ONPs in mice. Time course siRNA concentration in blood measured by FMT-CT after ONP injection (n= 3, 3 nmol of Cy5-siRNA). Cy5 labeled siRNAs are used in this experiment to determine the blood half-life of ONPs when I.V. injected. Estimated half-life of ONPs is 24.2 min and it is four times longer than the half-life of siRNA alone (~ 6 min)⁴.

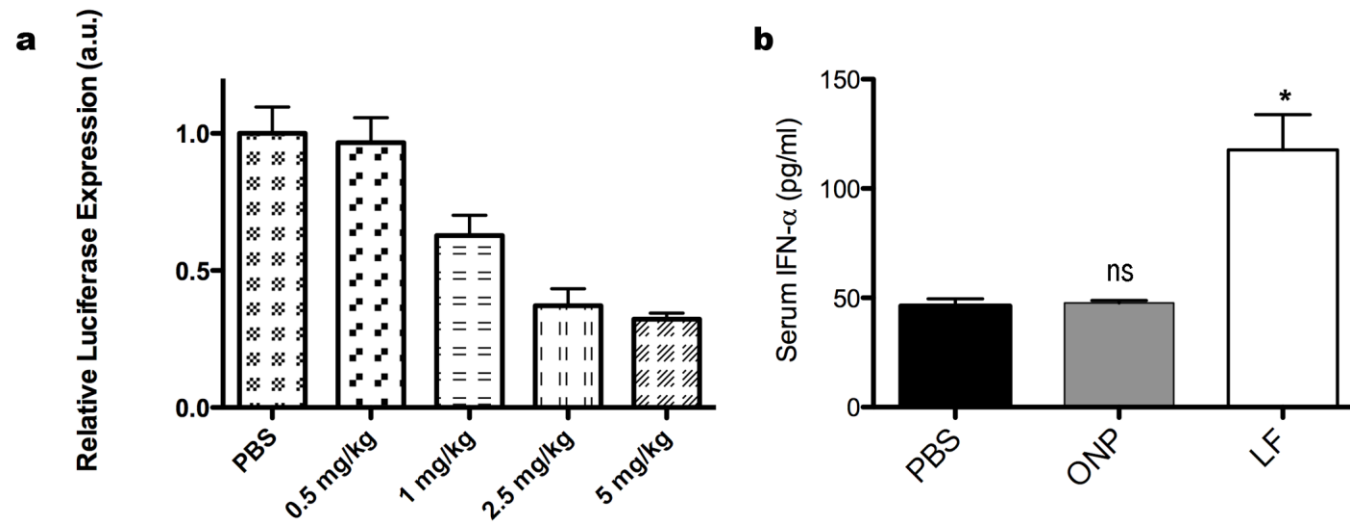


Figure S5 | In vivo characteristics of ONPs. **a.** Luciferase silencing as a function of dose by systemic injection of ONPs (n=5, PBS: Control PBS injection, injection dose shown in mg of siRNAs per kg of mouse). Anti-Luc ONPs exhibit $IC_{50} \sim 1.8$ mg/kg. **b.** Analysis of serum immune response for ONPs from in vivo study (n=3, PBS: Control PBS injection, ONP: ONPs with folate conjugated anti-Luc siRNAs, LF: Lipofectamine RNAiMax with folate conjugated anti-Luc siRNAs, ns=not significant, * $p < 0.006$). ONPs do not induce serum IFN release as compared with LF (over two-fold increase).

References

1. Goodman, R.P. et al. Rapid chiral assembly of rigid DNA building blocks for molecular nanofabrication, *Science* **310**, 1661-1664 (2005).
2. Nahrendorf, M. et al. Hybrid PET-optical imaging using targeted probes, *Proc. Natl. Acad. Sci. USA* **107**, 7910-7915 (2010).
3. Love, K.T. et al. Lipid-like materials for low-dose, in vivo gene silencing, *Proc. Natl. Acad. Sci. USA* **107**, 1864-1869 (2010).
4. Soutschek, J. et al. Therapeutic silencing of an endogenous gene by systemic administration of modified siRNAs. *Nature* **432**, 173-178 (2004).